Supplementary Information for

Structure-based design of a broadly protective influenza hemagglutinin stem immunogen

De-Jian Liu[1,13,14], Yan-Xia Ru[2,14], Shi-Long Zhao[1], Guo-Huan Yang[3,4], He-Ping Zheng[5], Cui-Cui Liu[1], Da-Long Yi[8], Xiao-Nuo Teng[9], Wen-Long Cao[9], Yi-Bo Tang[1], Wen-Wen Song[1], Xiao-Jun Li[10], Zhi-Fei Zhan[10], Xiu-Qin Zhong[11], Ya-Xuan Peng[12], Mu-Yang Wan[1], You-Song Peng[5], Xing-Yi Ge[1], Wen-Shuo Zhou[3,4], Wei-Guo Jia[3,4], Sen-Fang Sui[2,6,7], Yao-Wang Li[2] ✉ & Lei Deng[1] ✉

Corresponding author emails: ldeng@hnu.edu.cn (L.D.); liyw@sustech.edu.cn (Y.W.L.).

The PDF file includes:

Methods

Extended data figures and tables

References

Methods

Study design

In this study, our objective was to develop a soluble trimeric H1 stem-only immunogen without the exogenous trimerization motif, which can demonstrate cross-protective in the mouse model against heterologous influenza virus infection. The rational design of the H1 stem immunogen was initiated with the NC99 H1 protein and involved multiple rounds of mutation and variant screening processes. The oligomeric state and antigenicity of H1 stem variants were assessed using SDS-PAGE, immunoblotting, SEC, and ELISA methods. Five bnAbs recognizing different epitopes were included in binding tests to validate over antigenicity. Further characterization of the best-performing construct included bio-layer interferometry (BLI) for examining affinity to bnAbs, differential scanning fluorimetry (DSF) for measuring protein stability, negative-stain EM for assessing protein homogeneity, and cryo-EM for solving protein structure at atomic resolution. Provided a high-resolution structure model is obtained, we can explicitly analyze the antigen conformation and antigen/antibody Fab interaction approach, which is crucial for immunogen design. The effects of dosages and adjuvants on vaccine immunogenicity and vaccine cross-protection efficacy were evaluated through BALB/c mice immunization and viral challenge experiments. Additionally, total serum IgG titers and subclasses thereof as well as IgG cross-reactivity were measured; multiple serum antiviral mechanisms were evaluated, including virus cross-neutralization, hemagglutination inhibition, ADCC, neuraminidase inhibition, and inhibition of HA-mediated membrane fusion; mouse lung virus titers and hematoxylin and eosin staining on mouse lung sections were examined.

Structure-based rational design of trimeric H1 stem-only immunogen

The amino acid sequence of H1 from the NC99 H1N1 strain served as the template for the design of a stable soluble H1 stem trimer protein. A high-resolution protein structure model of H1 (PDB ID: 5UGY) from the A/Solomon Island/3/2006 H1N1 strain was utilized for structural analysis throughout the iterative process of the H1 stem protein design. Visualization and simulation of molecular structures were performed using the following software tools, PyMOL Version 3.0.3, UCSF ChimeraX Version 1.5, and Coot CCP4-7 v0.8.9.2. The probability distribution of the backbone dihedral angle for a specific amino acid substitution in the NC99 H1 stem was analyzed and visualized using the Ramachandran plot. The iterative design process consists of five steps, with phased design objectives progressively improving protein structure. Such an approach is cost-effective compared with generating a mega-size mutant library containing all possible combinations of mutations.

In the initial design, we generated a few mutant constructs bearing mutations as described below. The residue numbers of key site mutations are shown in Extended Data Fig. 1. The head domain was removed by deleting the fragment of S36 - K304, and then two ends at the deletion site were connected by a short linker 4×Gly. The transmembrane and cytosolic domains (I186-I222) were replaced with a factor Xa cleavage site (IEGR) for the removal of the purification tag and a hexa-His tag for affinity purification. The fusion peptide cleavage site was removed by a site mutation R326Q to prevent adventitious cleavage[24]. In addition, after head removal, exposed hydrophobic residues would disrupt stable conformation and also affect protein solubility, necessitating further optimization. To address this issue, we referred to the miniH1 design work conducted by Antonietta Impagliazzo et al.[15] and subsequently identified specific amino acids for substitutions,

including F63Y, V66I, L73S, I320K, and I323K. Given the high homology (~ 99%) between the amino acid sequences of the stem domains derived from both NC99 H1 (GenBank: AGQ47728.1) and A/Brisbane/59/2007 (H1N1) H1 (GenBank: ACA28844) that served as the template for designing miniH1 #4900, we inferred that these mutations would be reliable and beneficial to the NC99 H1 stem construct as well. Removal of the head and transmembrane domains inevitably destabilizes the remaining structure. To compensate for the loss of structural supports, we intended to introduce a pair of cysteine mutations that have been shown to effectively form interprotomer disulfide bonds in the stem region of the FL PR8 H1[47]. Therefore, we selected residues L20 and G47, along with several residues in their vicinity, for mutation into cysteines. The performance of protein mutants generated in this round falls short of expectations in all measures. All amino acid substitutions in the representative protein mutant #4 are illustrated schematically in Fig. 1.

The low binding activity of #4 to CR9114 indicates a priority to repairing intraprotomer antigenic conformation, which is crucial for inducing most bnAbs. Through meticulous analysis of the H1 stem structure, we identified 16 pairs of residues to be mutated into cysteines for building intraprotomer disulfide bonds. Then, these mutants were subjected to screening in expectation of obtaining a construct with restored antigenicity to CR9114. Among the round II protein mutants, only #16 demonstrated appreciable improvement in the antigenicity over the previous constructs, albeit primarily forming dimers.

The subsequent multiple rounds of mutation mainly aim to boost trimer formation. We previously analyzed several FL H1 structures and identified potential sites for cysteine mutations, attempting to establish interprotomer disulfide bonds[32]. According to this analysis result, a total number of 36 protein mutants were constructed by introducing different pairs of cysteines for the round III screening. In this round, #31 exhibited superior properties, in terms of enhancing antigenicity, expression level, and trimer formation. The polypeptides of #31 covalently form dimers, trimers, and disordered aggregates. The presence of covalent trimers implies that either the cysteine pair L20C/G47C, G1C/S124C, or both of them could form the intended interprotomer disulfide bonds.

Augmenting the hydrophobicity of the protomer interface will further enhance the propensity for trimerization, thereby facilitating efficient formation of the covalent trimers. As per the design strategy described in the main text, space-filling with hydrophobic amino acids is favored to address this issue. Ideally, this approach will spatially align the monomers of the H1 stem as observed in homo-trimer architecture. In round IV of screening, #31 was used as a template for generating protein mutants. Several hydrophilic residues (N95 and R106 from the CD helix, along with K51 and E103 from a pH-sensitive switch domain) were individually or collectively selected for mutation into hydrophobic residues. A total of 150 mutants containing various mutations were constructed for screening. Experimental results confirm the effectiveness of the space-filling strategy applied in the design of the H1 stem protein, as evidenced by construct #184 bearing N95I substitution that resulted in a substantial increase in trimer proportion. At this stage, we also attempted to establish additional metal-coordination bonds or salt bridges at certain potential sites, using several templates including #31 as well, but these efforts did not lead to an increased trimer yield.

We further optimized the trimer interface by substituting more hydrophobic amino acids for M77 and/or V84 in #184. A total number of 25 protein mutants were generated for screening in round V. Finally, we found that the substitution M77I miraculously led to the almost complete formation of trimers and the resulting protein mutant #219 demonstrated superior stability and antigenicity.

Propagation of influenza viruses

Fertile chicken eggs were employed to produce large amounts of influenza A and B virus strains used in this study, including PR8, NJ76, X-179A, A/Sichuan/SWL1/2009 (SC09, H1N1), A/Hong Kong/8/1968 (HK68, H3N2), A/Guizhou/54/1989 (GZ89, H3N2), B/Ibaraki/2/1985 (IB85), B/Anhui-Tunxi/1528/2014 (AH14), and B/Brisbane/1/2007 (BRS07). The SPF-grade fertilized chicken eggs were incubated at 37 ℃ with 60% humidity. On the ninth day after fertilization, egg candling was conducted using a flashlight to assess embryo growth. On the tenth or eleventh day, the eggs were transferred into the biosafety level 2 (BSL-2) laboratory for virus inoculation experiments, in which 200 μl of virus solution at a concentration of 10^4 plaque forming unit (pfu)/ml was injected into the allantoic cavity using a needle. After two days of incubation at 37 °C, the eggs were chilled at 4 °C for at least 4 hours (hrs). The eggshell above the air sac and the chorioallantoic membrane were then carefully opened using sterile tweezers to collect the allantoic fluid containing the virus. The fluid was cleared from debris by centrifugation at 10,000 × g, at 4 °C for 10 minutes (min), and pelleted by ultracentrifugation at 140,000 × g, at 4 °C for 2 hrs. The pelleted virion particles were resuspended in cold sterile PBS on ice, then further purified using a 15%-30%-45%–60% discontinuous sucrose gradient ultracentrifugation at the speed of 140,000 × g, at 4 °C for 2 hrs. The sucrose layer containing virions was collected and resuspended in ice-cold sterile PBS. The influenza virus samples were dialyzed twice against sterile ice-cold PBS at 4 °C for 1 hr, aliquoted, and transferred to -80 °C for long-term storage. The median tissue culture infective dose ($TCID_{50}$) and/or the mouse median lethal dose (mLD_{50}) for these viruses were titrated using the Madin-Darby canine kidney (MDCK, ATCC) cell line and the BALB/c mouse strain, respectively; subsequently, the results were calculated using the Reed and Munch method[48].

Expression, purification, and preliminary characterization of recombinant proteins

The Bac-to-Bac baculovirus expression system was employed as a reliable way to produce recombinant proteins including H1 stem mutants, soluble FL HAs, and IgG antibodies. The NC99 FL H1 amino acid sequence (GenBank protein ID: AFO65027.1) was selected as the template for engineering the H1 stem proteins. NC99 H1 bears a Factor Xa-preferred cleavage site and a hexa-His tag at the C-terminus. The encoding nucleotide sequence was optimized based on the codon preference of Sf9 insect cells to achieve high-level expression and then inserted into the multiple cloning site in the pFastBac-1 vector to facilitate recombinant bacmid preparation and site-directed mutagenesis operations. The Sf9 insect cell line was utilized for the recombinant baculovirus generation and protein expression. Recombinant H1 stem mutants were purified through affinity chromatography employing Ni-NTA resin and subsequently their molecular weights and purities were assessed by SDS-PAGE and Western blotting. Selected H1 stem mutant candidates underwent further analysis of protein yields and their molecular weights by SEC using a Superdex 200 Increase 3.2/300 GL column. The #219 trimer proteins treated or untreated with the peptide N-glycosidase F amidase (Beyotime) were subjected to SDS-PAGE and Coomassie blue staining analysis. The #219 trimers enzymatically cleaved by the Factor Xa protease were separated from the hexa-His tag and the protease by SEC and then used for immunization.

A variety of soluble recombinant FL HA proteins were used in ELISA for titrating specific serum antibodies. The NC99#2 H1 trimer protein (modified from the H1 sequence of the NC99 H1N1

strain; GenBank accession number: AFO65027) and the WA11#5 H1 trimer protein (modified from the H1 sequence of the A/Washington/5/2011 H1N1 strain; GenBank accession number: AGK72598) were previously developed by our group and purified by SEC for use in this experiment, both of which are stabilized by introduced interprotomer disulfide bonds and do not contain exogenous trimerization motifs[32]. Additional soluble recombinant FL HA proteins were designed based on HA sequences from various influenza A viruses, including the A/Michigan/45/2015 H1N1 strain (MG15; GenBank accession number of H1: APC60198.1), the A/Wisconsin/588/2019 H1N1 strain (WIS19; GISAID accession number of H1: EPI1661758), the A/Shanghai/202/1957 H2N2 strain (SH57; GenBank accession number of H2: AIY59285.1), the A/Hong Kong/1/1968 H3N2 strain (HK68; GenBank accession number of H3: AFG71887.1), the A/Hong Kong/4801/2014 H3N2 strain (HK14; GISAID accession number of H3: EPI834581), the A/Darwin/6/2021 H3N2 strain (DW21; GISAID accession number of H3: EPI_ISL_4551091), the A/Hong Kong/483/97 H5N1 strain (HK97; GenBank accession number of H5: AF046097.1), the A/Viet Nam/1203/2004 H5N1 strain (VN04; GenBank accession number of H5: ABP51977.1), the A/Chongqing/02/2021 H5N6 strain (CQ21; GISAID accession number of H5: EPI_ISL_4568644), the A/Jiangsu/NJ210/2023 H5N1 strain (JS23; GISAID accession number of H5: EPI_ISL_17075747), the A/Shanghai/2/2013 H7N9 strain (SH13; GenBank accession number of H7: YP_009118475.1), the B/Florida/4/2006 strain (FLD06; GenBank accession number of HA: ACA33493.1), and the B/Colorado/22/2017 strain (CLD17; GenBank accession number of HA: ATP83052.1). These proteins incorporate a T4 foldon motif sequence for trimerization of the FL HA and a hexa-His tag at the C-terminus for purification. The expression of these recombinant HA proteins was achieved using the baculovirus expression system, followed by purification through affinity chromatography using Ni-NTA resin.

The construction of recombinant heavy and light chains of the five bnAbs was described previously[32]. Briefly, the heavy and light chains bear an N-terminal melittin signal peptide and an N-terminal GP64 signal peptide, respectively. All constant regions of these recombinant bnAbs were derived from the human IgG1 subclass. The recombinant bnAbs were expressed from Sf9 insect cells and were purified by protein A affinity chromatography followed by an additional SEC purification.

ELISA

The binding activities of HA stem protein mutants to bnAbs were assessed by performing ELISA. The 96-well clear polystyrene microplates were coated with bnAbs, including CR9114, CR6261, CT149, 3I14, and FISW84, at the concentration of 100 ng per well, and incubated overnight at 4 ℃. Subsequently, the microplates were blocked with 300 μl per well of 10% (w/v) skim milk in PBST (PBS containing 0.1% Triton X-100 detergent) at 37 ℃ for 1 hr, and then incubated with H1 stem protein mutant samples that were 3-fold serially diluted starting from the concentration of 3 μg/ml at 37 ℃ for 1 hr, followed by three washes with PBST, 5 min each time. A hundred μl of 10 μg/ml anti-His goat-anti-human secondary antibody conjugated with horseradish peroxidase (HRP) were added to each well and the plates were incubated at 37 ℃ for 1 hr. After three washes with PBST, 50 μl of the color-developing solution containing 3,3'5,5'-Tetramethylbenzidine (TMB, Thermo Fisher Scientific) substrate was added to each well. The reaction was stopped by adding 50 μl of 1 M H_2SO_4 each well, then the absorbance was read at 450 nm using a microplate reader. Areas under the curve (AUC) values were calculated based on the titration curves using GraphPad Prism 8.0 software (GraphPad Software, San Diego, CA, U.S.).

Serum antibody titers were determined by ELISA where the plates were coated with formalin-inactivated influenza A viruses and soluble HA antigens at the concentrations of 500 ng per well and 100 ng per well, respectively. The serum sample from each mouse (n = 5 per group) was 3-fold serially diluted for antibody titration. In serum cross-binding experiments, the pooled serum samples of each group were assayed in ELISA. Antibody titers of total IgG and subclasses of IgG1, IgG2a, and IgG3 were measured by incubation with secondary antibodies HRP-conjugated goat-anti mouse IgG, HRP-conjugated goat-anti mouse IgG1, HRP-conjugated goat-anti mouse IgG2a, and HRP-conjugated goat-anti mouse IgG3, respectively (Proteintech Group, Inc.).

BLI assay

The kinetics and affinity of interactions between the H1 stem protein #219 and HA stem-specific bnAbs were assessed using BLI assay. The load bnAb molecules including CR9114, CR6261, 3I14, and CT149, were diluted to the concentration of 5 μg/ml in PBST, and the antibodies were immobilized on ProA bio-sensors (Octet Sartorius), respectively. Then, serial dilutions of the #219 protein in PBST solution at the concentrations of 57.5nM, 28.7nM, 14.4nM, 7.18nM, and 3.59nM, were subjected to BLI analysis. The binding kinetics were analyzed with the Octet Analysis software v12.0 package.

Preparation of immune complexes

We intended to characterize the protein structures of both the #219 trimer protein and the #219/Fabs immune complexes as well by utilizing negative-stain EM and cryo-EM. The Fab fragments were isolated through enzymatic cleavage of IgG1 bnAbs CR9114, FISW84, and CT149, using papain (Yeasen Biotechnology, Inc.). Briefly, papain was dissolved in PBS containing 20 mM L-cysteine and was activated in a 37 °C water bath for 20 min. Each IgG1 antibody sample was mixed with the papain solution, at an antibody-to-papain mass ratio of 50:1, and was incubated at 37 °C for 3 hrs. Then, the iodoacetamide (Sigma-Aldrich) was added at a final concentration of 30 mM, and the mixture was incubated at room temperature in the dark for 40 min to terminate the reaction. Papain digestion of IgG1 generates two Fab fragments and one Fc fragment. The Fab fragments were purified by excluding the Fc fragments and trace of intact IgG1 using Protein A resin, and further by removing the papain and iodoacetamide using a prepacked Superdex 200 Increase 3.2/300 column (Cytiva). The pure Fab fragments derived from CR9114, FISW84, and CT149 were obtained and used for the preparation of the #219/Fab immune complexes.

To obtain the #219/Fab immune complexes, the SEC-purified #219 trimer protein was incubated with the Fab fragments derived from CR9114, CR9114/FISW84, and CT149, respectively, at an antigen-to-Fab molar ratio of 4:1, at 37 °C for 2 hrs. Next, these complexes were purified by SEC using a Superdex 200 Increase 3.2/300 column and the PBS elution buffer (pH 7.4). The purified immune complexes were concentrated by using centrifugal filter tubes (Merck) and were directly used for EM analyzes or stored at -80 °C for later use.

Negative-stain EM analysis

Five μl of the purified #219/Fab immune complexes at a concentration of 0.01 mg/ml in PBS (pH 7.4) were carefully applied onto a glow-discharged continuous carbon film grid. Excess liquid was

then removed by blotting with filter paper. Subsequently, the protein samples were double-stained at room temperature by applying 4 µl of 2% w/v uranyl acetate and blotting dry with filter paper after 10 and 6 seconds, followed by air drying. Finally, the grids were imaged at 73,000× magnification (corresponding to a calibrated pixel size of 1.93 Å/pixel) using a Talos 120C transmission electron microscope equipped with a Ceta 16M detector (Thermo Fisher) at an accelerating voltage of 120kV.

Cryo-EM grid preparation

The 300 mesh Quantifoil Cu R1.2/1.3 GO grid was subjected to glow discharge at 10 mA for 15 seconds. Subsequently, 4 µl of each protein complex sample at a concentration of 0.07 mg/ml was carefully dispensed onto the grid in the Vitrobot (Thermo Fisher), where the temperature and humidity were precisely set to 8 °C and 100%, respectively. The grid was then delicately blotted with a nominal blot force of 1 and immediately plunged into pre-cooled liquid ethane for vitrification.

Cryo-EM data collection

Cryo-EM data was obtained using a 300 KV FEI Titan Krios transmission electron microscope (TEM) equipped with a K3 summit direct detector, a Gatan Continuum (1069) EELS energy filter, and a spherical aberration corrector. Automated data acquisition was carried out with SerialEM software at a magnification of 130,000× in super-resolution mode (yielding a pixel size of 0.46 Å). A series of 32 frames movies was collected within a defocus range from 1.5 to 2.5 µm, with a total electron dose of 50 $e^-/Å^2$ (equivalent to 1.56 $e^-/Å^2$ per frame), which resulted in a total of 3,946 non-tilt movies and 1,131 25°-tilted movies (Extended Data Table 2).

Cryo-EM data processing

MotionCorr2 was employed to align the acquired movie frames, addressing beam-induced motion and producing dose-weighting micrographs that were binned by 2, having a pixel size of 0.92 Å. All subsequent steps were performed in cryoSPARC4.4. The software's Patch CTF program estimated the defocus value for each micrograph. From a selection of 400 micrographs, particles were identified using the Blob pick program, with a focus on those exhibiting high signal-to-noise ratios (SNR). A rapid 2D classification process facilitated the cleaning of the stack by categorizing particles into distinct classes and removing unsuitable ones. These refined 2D classes served as templates for further particle detection via the Topaz program. Ahead of training a model for particle extraction, all micrographs were processed with Topaz's denoise function. An initial model was established from these particles using the Ab-Initio reconstruction method.

Utilizing the Topaz extract feature, particles were then obtained, with the process emphasizing the retention of high-SNR 2D classes through 2D classification, yielding a significant quantity of particles: 207,801 from non-tilted micrographs and 34,912 from 25°-tilted micrographs. Utilizing the initial model, the non-tilt micrograph particles were used to construct a new reference through Homogeneous Refinement. This led to the acquisition of a 3.91 Å-resolution map, further refined to 3.83 Å for the particles from the 25°-tilted micrographs. The resolution was enhanced to 3.59 Å by applying Global CTF Refinement and introducing C3 symmetry.

Addressing the trimer's inherent flexibility, a focused approach was taken by masking out the asymmetric unit and engaging the symmetric extension function, effectively tripling the particle count and achieving a refined map at 2.97 Å-resolution. This iterative and meticulous approach underscores the precision and adaptability of the used algorithms and tools in enhancing the resolution and quality of the structural data obtained via cryo-electron microscopy (Extended Data Fig. 10).

Addressing preferred orientation

The serious preferred orientation problem was observed in the samples of #219/CR9114 Fab complex, #219/CT149 Fab complex, and #219/3I14 Fab complex. Based on our assumption of counterbalancing the gravity center of the immune complex, by analyzing the epitope footprints of the currently available bnAbs, we employed the CR9114 Fab and FISW84 Fab, both of which recognize nonoverlapping epitopes, to simultaneously bind the #219 trimer protein. Consequently, the #219/CR9114 Fab/FISW84 Fab complex no longer exhibited serious particle orientation bias in preferred orientation problem. In addition, spIsoNet and cryoPROS programs[49] noticeably enhanced the map quality further (Extended Data Fig. 10).

Model building

A monomer structure of the #219/CR9114 Fab/FISW84 Fab complex was predicted by AlphaFold2 and then was fitted into the high-resolution map visualized in the ChimeraX as the initial model. Subsequently, the initial model was improved and refined by using the Coot program and the Phenix program (Extended Data Table 2). A psesudo-C3 symmetry model was also generated base on this monomer model.

DSF assay

DSF offers a rapid and sensitive method for measuring protein thermal stability. The thermal denaturation of the SEC-purified #219 trimer protein and #184 trimer protein is determined using the Applied Biosystems 7500 rapid real-time fluorescent quantitative PCR system (Thermo Fisher). The SYPRO Orange dye (Thermo Fisher) was used for DSF. In the 20 μl reaction system, the proteins were diluted to a final concentration of 0.1 mg/ml. The scan is programmed to initiate at 25 °C, followed by a temperature gradient with a heating rate of 1 °C per minute until reaching a final temperature of 99 °C. The PBS solution without protein samples served as the negative control. An increase in the Tm is interpreted as an augmentation in protein thermal stability.

Vaccination and viral challenge experiments

The proposal for all mice experiments was reviewed and approved by the Animal Ethics Committee from the College of Biology, Hunan University. (Ethics File Code: HNUBIO202202001). All animal experiments were performed in strict accordance with the local animal welfare legislation. The protein solution underwent sterile filtration prior to the formulation of adjuvanted vaccines. In the immunization experiments described below, specific-pathogen-free female BALB/c mice (6 – 8 weeks old, n = 5 – 8 per group) received intramuscular immunizations in their hind legs three times at 3-week intervals. Only mice in the QIV immunization group were

administered 2 doses of the vaccine at 3-week intervals. Mouse blood samples were collected from the submandibular vein one day prior to the prime immunization (preimmune) and two weeks after each immunization. The challenge experiments involving influenza viruses were carried out in a biosafety level 2 animal facility, and three weeks after the final immunization, intranasal infections of mice were conducted under ketamine/xylazine anesthesia.

To assess the immunogenicity of #219 protein, groups of 5 mice were administered with five different doses (1 μg, 5 μg, 10 μg, 25 μg, and 50 μg of #219 protein in 50 μl sterile PBS), each of which was emulsified with 50 μl of AddaVax (InvivoGen). Several commonly used experimental adjuvants were evaluated in mouse immunization to optimize the immunogenicity of #219. Groups of 5 mice were vaccinated with 10 μg of #219 formulated with Aluminum hydroxide (InvivoGen), Sigma Adjuvant System (Sigma-Aldrich), AddaS03 (InvivoGen), and AddaVax, respectively. AddaVax and AddaS03 are squalene-based oil-in-water nano-emulsions with a formulation similar to that of the licensed adjuvants MF59 and AS03, respectively. A negative control group was mock-immunized with an equal volume of sterile PBS. The serum samples collected two weeks after each immunization were analyzed for H1-specific antibody titers using ELISA. To evaluate the efficacy of vaccine protection, all immunized mice were challenged by intranasal infection with a lethal dose 8 × LD_{50} of NJ76 three weeks after the second booster. Mice were monitored daily for changes in survival rates and body weights for 14 days following influenza infection.

We conducted immunization and viral challenge experiments to compare the cross-protection efficacies of the #219 immunogen and the split QIV (GDK Biotechnology, Taizhou, China) recommended for the northern hemisphere 2022 - 2023 influenza season by World Health Organization, which contains HA and NA antigens from an A/Victoria/2570/2019 (H1N1)pdm09-like virus, an A/Darwin/9/2021 (H3N2)-like virus, a B/Austria/1359417/2021 (B/Victoria lineage)-like virus, and a B/Phuket/3073/2013 (B/Yamagata lineage)-like virus. Groups of 8 mice were immunized with 10 μg of #219 protein, diluted QIV containing 4 μg of HA antigens, 10 μg of homologous IIV serving as a positive control, and an equal volume of 50 μl of sterile PBS serving as a negative control. Each dose of all these vaccines was emulsified with 50 μl of AddaVax in immunization experiment. The serum samples collected two weeks after the last immunization were subjected to ELISA analysis for assessing serum cross-reactivity towards various HA proteins. Three weeks after taking the last dose of vaccine, groups of immunized mice (n = 5 per group) were intranasally infected with a lethal dose of 8 × LD_{50} of diverse heterologous H1N1 viruses, including ~ 238 pfu of PR8 (1934), ~ 1.39 × 10^7 pfu of NJ76 (1976), and ~ 508 pfu of X-179A (H1 thereof derived from a pdm2009 strain). Mice were monitored daily for changes in survival rates and body weights for 14 days following influenza infections.

Mouse lung virus titration assay and lung histological analysis

Mice (n = 3 per group) from immunization groups of #219, PR8 IIV, and PBS, were euthanized 5 days after infection with 0.5 × LD_{50} of PR8. Likewise, mice (n = 3 per group) from immunization groups of #219, X-179A IIV, and PBS, were euthanized 5 days after infection with 0.5 × LD_{50} of X-179A. Three uninfected mice were euthanized as well for isolation of lung tissues to serve as negative control samples in the virus titration assay. Determination of lung virus titers in mice was described previously[50]. The titration of viruses in the supernatants of lung homogenate samples was performed by measuring hemagglutination activity, and the titers were calculated using the Reed and Muench method.

For histological analysis, three mice per immunization group were euthanized at day 5 after sublethal infection with 0.5 × LD_{50} of PR8 or X-179A. The freshly isolated lung tissues were fixed in 10% neutral buffered formalin and embedded in paraffin wax. Then, a series of ten μm-thick lung sections were prepared using a microtome, stained with hematoxylin and eosin, and then examined under a light microscope.

Virus neutralization assay

MDCK cells were seeded at a density of 30,000 cells per well in 96-well cell culture plates (Jet Bio-Filtration, Guangzhou, China), and incubated in a complete culture medium containing Dulbecco's Modified Eagle Medium (DMEM) supplemented with L-glutamine, 5% fetal bovine serum (FBS, Gibco), 100 U/ml penicillin, and 100 μg/ml streptomycin stock solution (Gibco) at 5% CO_2, 37 ℃ overnight. After the heat inactivation of serum samples at 56 ℃ for 30 min, the serum was serially diluted 2-fold, starting from a dilution of 1:10 in serum-free DMEM. The resulting serum dilutions were then combined with an equal volume of virus solution containing 100 × median tissue culture infectious dose ($TCID_{50}$) virus per 50 μl in DMEM, and these mixtures were incubated at room temperature for 1 hr. This assay encompassed various influenza virus strains, including PR8 H1N1, NJ76 H1N1, X-179A H1N1, SC09 H1N1, HK68 H3N2, GZ89 H3N2, B/IB85, and B/AH14. After three washes with sterile PBS, each well of MDCK cell culture was inoculated with 100 μl of the virus-serum mixture and incubated at 5% CO_2, 37 ℃ for 1 hr. Following washes with sterile PBS for three times, each well received an addition of 100 μl DMEM supplemented with L-1-Tosylamido-2-phenylethyl chloromethyl ketone (TPCK)-treated trypsin (Thermo Fisher Scientific) at a concentration of 2 μg/ml; thereafter the cell cultures were maintained under conditions of 5% CO_2, 37 ℃ for 48 hrs. Subsequently, the supernatants were subjected to a standard hemagglutination assay to evaluate viral inhibition activities.

Hemagglutination inhibition assay

Serum samples were mixed thoroughly with a 3-fold volume of receptor-destroying enzyme (RDE; Denka Seiken, Tokyo, Japan) solution, which is a neuraminidase from *Vibrio cholerae*, and the samples were incubated at 37 ℃ for 18 hrs, to eliminate non-specific binding of sialylated innate inhibitors in serum with viral HA, followed by addition of a 3-fold volume of 2.5% sodium citrate solution (w/v in distilled water) and heat inactivation at 56 ℃ for 30 min to deactivate the RDE. Subsequently, a 3-fold volume of 0.5% chicken red blood cell suspension (v/v in PBS) was added and incubated at room temperature for 30 min to remove non-specific hemagglutination substances, followed by spinning down and collecting the supernatant, resulting in a final 1:10 dilution of RDE-treated serum. Two-fold serial dilutions of the supernatant were prepared in quadruplicate, mixed with 4 hemagglutination units of each of influenza A viruses including PR8 H1N1, NJ76 H1N1, X-179A H1N1, SC09 H1N1, HK68 H3N2, and GZ89 H3N2, and the samples were incubated at room temperature for 1 hr. This was followed by the addition of 1% chicken red blood cells and further incubation at room temperature for 1 hr. The lowest serum dilution able to inhibit virus hemagglutination is shown.

ADCC reporter bioassay

MDCK cells were seeded in 96-well plates at a density of 2.5×10^4 cells per well and maintained in DMEM supplemented with 10% heat-inactivated FBS at 5% CO_2, 37 ℃ for 4 hrs. MDCK cell cultures were inoculated with 200 μl per well of influenza virus solution in serum-free media (SFM, Thermo Fisher) containing 2.5×10^5 pfu (MOI= 10) of PR8 and X179, respectively. The infection of MDCK cells was allowed to proceed for 24 hrs. Serum samples collected from the #219-immunized mice and the PBS mock-immunized mice were serially diluted 3-fold in assay buffer consisting of RPMI 1640 (Gibco) and 4% heat-inactivated FBS, and were then heat-inactivated at 56 °C for 30 min. Subsequently, 50 μl of each serum dilution was mixed with 25 μl of ADCC reporter cell suspension (a stable Jurkat cell line expressing a firefly luciferase reporter gene under the control of NFAT response elements with constitutive expression of mouse FcγRIV) at a density of 3×10^6 cells per ml and the mixtures were added to the infected cell cultures at a target/effector ratio of 1:3, followed by incubation at 5% CO_2, 37 °C for 6 hrs. Cell samples were equilibrated to ambient temperature for 10 min, and then 75 μl of Bio-Glo Luciferase Assay substrate reagent (Promega) was added to each well. The luminescence was promptly read out on a SpectraMax ID3 multimode microplate reader (Molecular Devices). Data are presented as fold induction of signal in the absence of serum.

Neuraminidase inhibition assay

Antisera were tested regarding their inhibitory effects on the viral NA activity by using a standard ELLA protocol as described previously[51]. Briefly, heat-inactivated sera were 10-fold diluted and incubated with an equal volume of 300 μg/ml formalin-inactivated H1N1 viruses, including PR8, NJ76, and X-179A, respectively, in PBS supplemented with 1% (w/v) BSA, 1 mM $CaCl_2$, 0.5 mM $MgCl_2$, 0.5% Tween-20, at 37 ℃ for 30 min. Virus-serum mixtures with 200 μl for each sample were applied to ELISA plates (Nunc Maxisorp) coated with 250 μg fetuin (Sigma-Aldrich) per well and incubated at 37 ℃ for 18 hrs. HRP-conjugated peanut agglutinin at the concentration of 5 μg/ml was used to detect the galactose residues exposed after NA cleaves off sialic acid from glycans on fetuin.

Membrane fusion assay

To test the inhibition effect of #219 serum samples on H1 fusogenicity, a cell-cell fusion assay was conducted. HEK293T cells were cultured in 24-well cell culture plates (Jet Bio-Filtration, Guangzhou, China) at 5% CO_2, 37 ℃ until reaching around 80% confluence. The cells were then co-transfected with the recombinant eukaryotic plasmid pCS2 expressing green fluorescent protein (GFP) and either pcDNA3.1 plasmid expressing NC99 FL H1 or an empty pcDNA3.1 plasmid as a negative control, using Lipofectamine 2000 transfection reagent (Thermo Fisher Scientific) according to the manufacturer's instructions. After transfection, the cells were cultured in DMEM containing 5% FBS and 2 μg/ml TPCK-treated trypsin at 5% CO_2, 37 ℃ for 24 hrs, and the green fluorescence in the cells detected using an inverted fluorescent microscope (Nikon, Japan). Serum samples collected from immunization groups of the PBS and #219, as well as preimmune serum samples, were heat-inactivated at 56 ℃ for 30 min to inactivate heat-labile complement proteins that could potentially interfere with experiment results. The heat-inactivated diluted serum samples (10-fold dilution using DMEM) were filter-sterilized through the 0.45 μm membrane filters

(Millipore). Following three washes with sterile PBS, each well of the cell cultures was treated with 200 μl of these serum samples and incubated at 5% CO_2, 37 ℃ for 1 hr. After three washes with sterile PBS, the cell cultures were incubated in DMEM at pH 5.0, at 5% CO_2, 37 ℃ for 10 min, to induce conformational changes in H1 proteins to postfusion. Treatment of cell culture with DMEM at pH 7.4 served as the negative control in membrane fusion experiments. Subsequently, the cells were washed with sterile PBS three times, and cultured in complete culture medium at 5% CO_2, 37 ℃ for 1 hr to allow the cytoskeleton rearrangements involved in syncytia formation. The morphology of cells expressing GFP was visualized by fluorescence microscopy.

Statistical analysis

All data plotted with error bars are expressed as means with SD. Statistical analyses were performed using the GraphPad Prism 8.0 software. The statistical significance of the survival rates was analyzed by Log-rank Mantel-Cox test, the statistical significance of the percentages of initial body weight between groups was analyzed by two-way ANOVA, while the ELISA, lung viral load, and ELLA data were analyzed by an unpaired two-tailed *t*-test. A *p*-value less than 0.05 was considered to be significant.

Extended data figures and tables

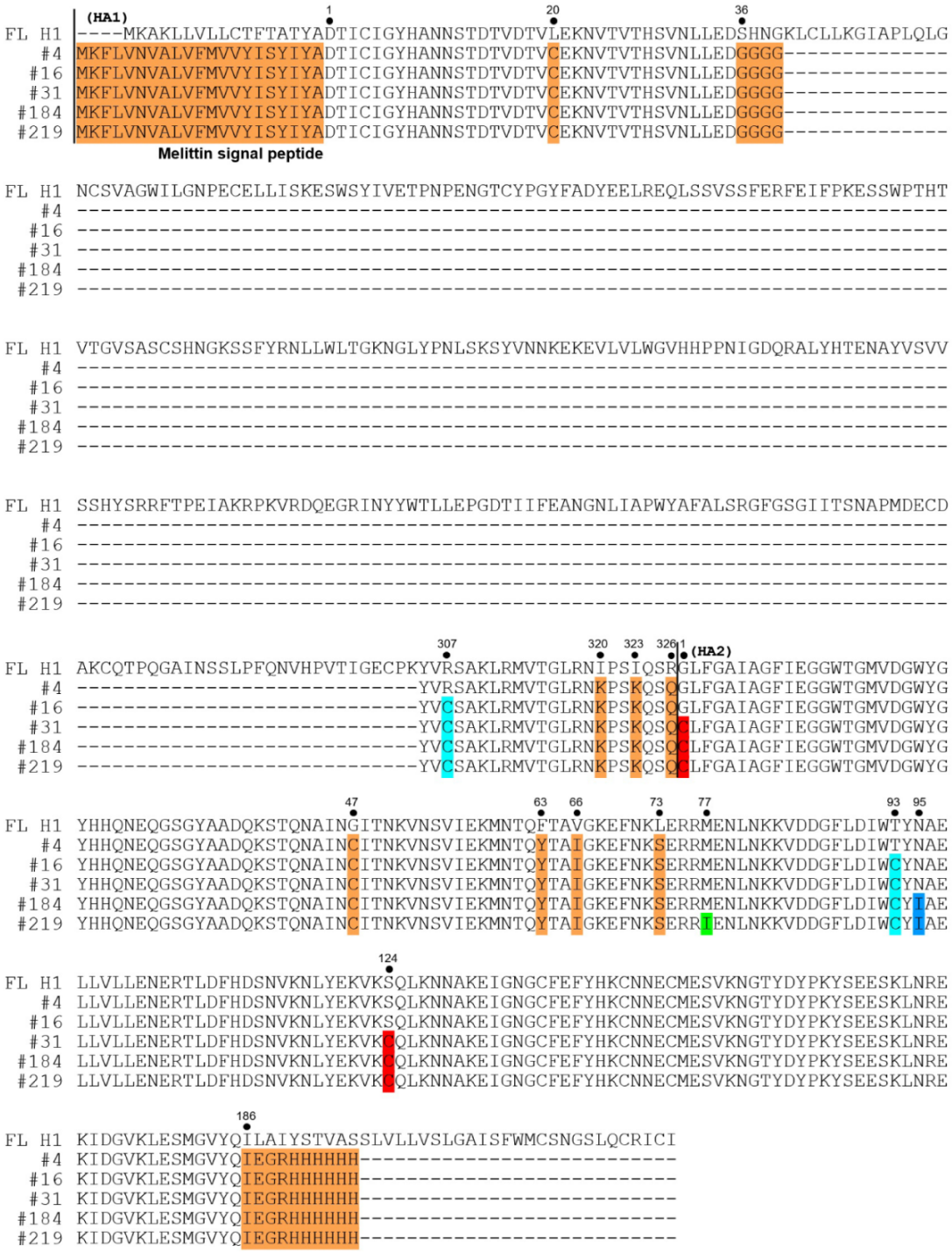

Extended Data Fig. 1. Amino acid sequence alignment of FL H1 and H1 stem variants. FL H1 sequence is derived from the NC99 H1N1 strain. Amino acid residue numbering of the HA1 peptide begins from the Aspartic acid residue closely behind the signaling peptide sequence, while that of the HA2 peptide begins from the Glycine residue after the fusion peptide sequence. The amino acid substitutes are differentially colored in the sequences of H1 stem constructs for each round of mutation.

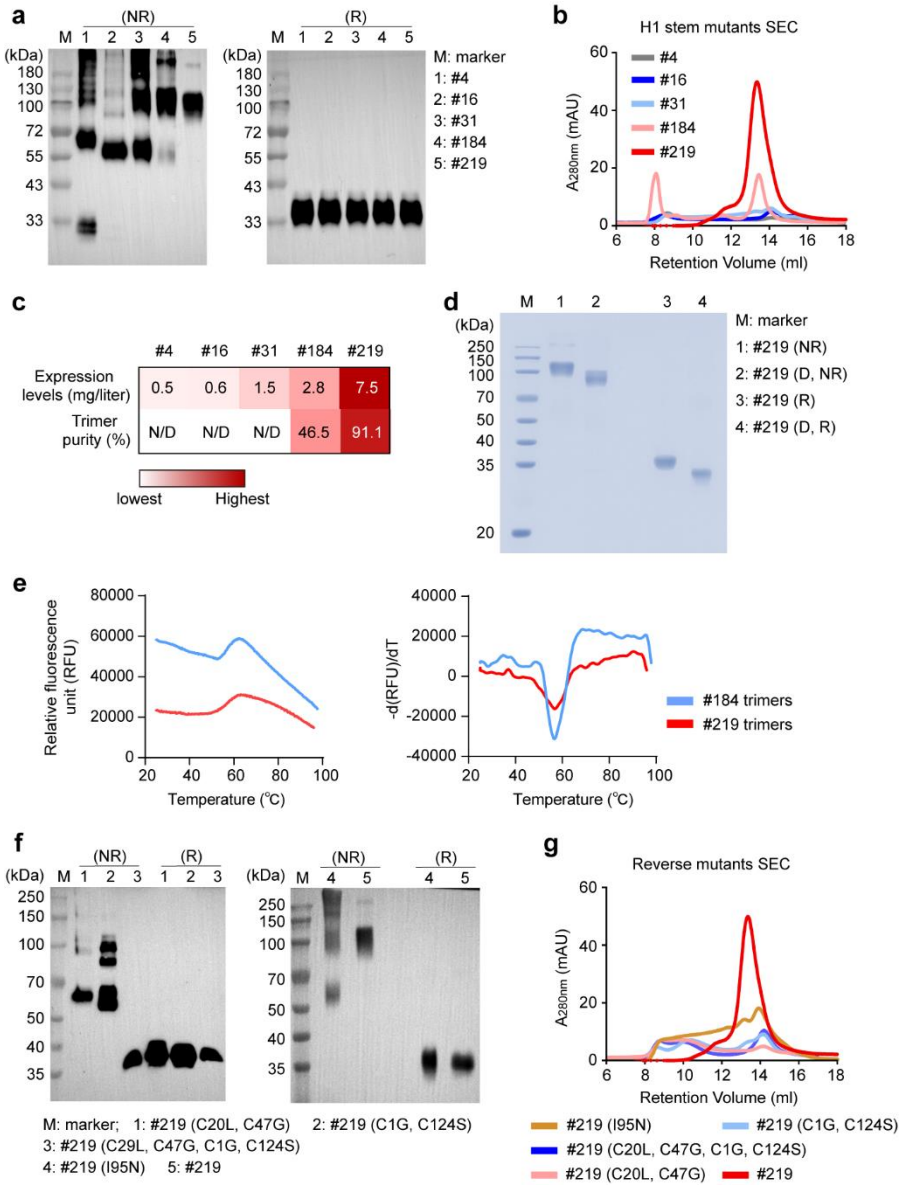

Extended Data Fig. 2. Characterizations of selected H1 stem variants. a, Western blot analysis of selected H1 stem variant candidates from each round of mutation, under non-reducing (NR) and reducing (R) conditions. **b**, SEC traces of the same candidates as analyzed in panel (A). **c**, A heatmap illustrates the expression yields defined by the amount of affinity-purified protein per liter of culture and trimer purity of the selected #184 and #219 mutants. N/D indicates not determined. It is difficult to discriminate the trimer peak from the SEC curves of #4, #16, and #31, thus, their trimer purities were not determined. **d**, The #219 protein and its deglycosylated (D) protein were analyzed by using SDS-PAGE under NR and R conditions and Coomassie blue staining. **e**, Melting curves and derivative plots for the determination of melting temperature (Tm). The Tm values of the SEC-purified trimer proteins of #184 and #219 are 56.62 °C and 57.72 °C, respectively. **f**, Western blot analysis of #219 and back mutant proteins under NR and R conditions. **g**, SEC traces of #219 and back mutant proteins.

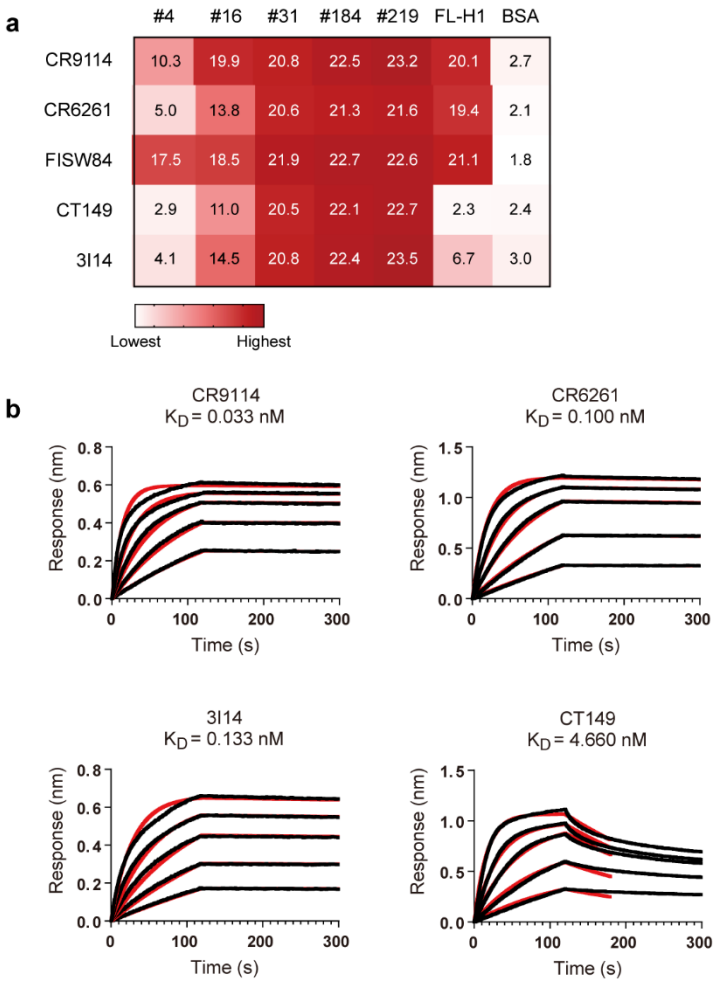

Extended Data Fig. 3. Antigenicity assessment of selected H1 stem variants. a, The binding activities of H1 stem variants to five bnAbs are represented in a heatmap. The AUC values shown within the boxes signify the binding activity. The y-axis represents the bnAbs utilized for binding, and the labels atop indicate the antigens used to coat the ELISA plates, encompassing the selected variant candidates and the BSA control protein. **b**, Real-time detection of bindings of #219 to CR9114, CR6261, 3I14, and CT149 by biolayer interferometry.

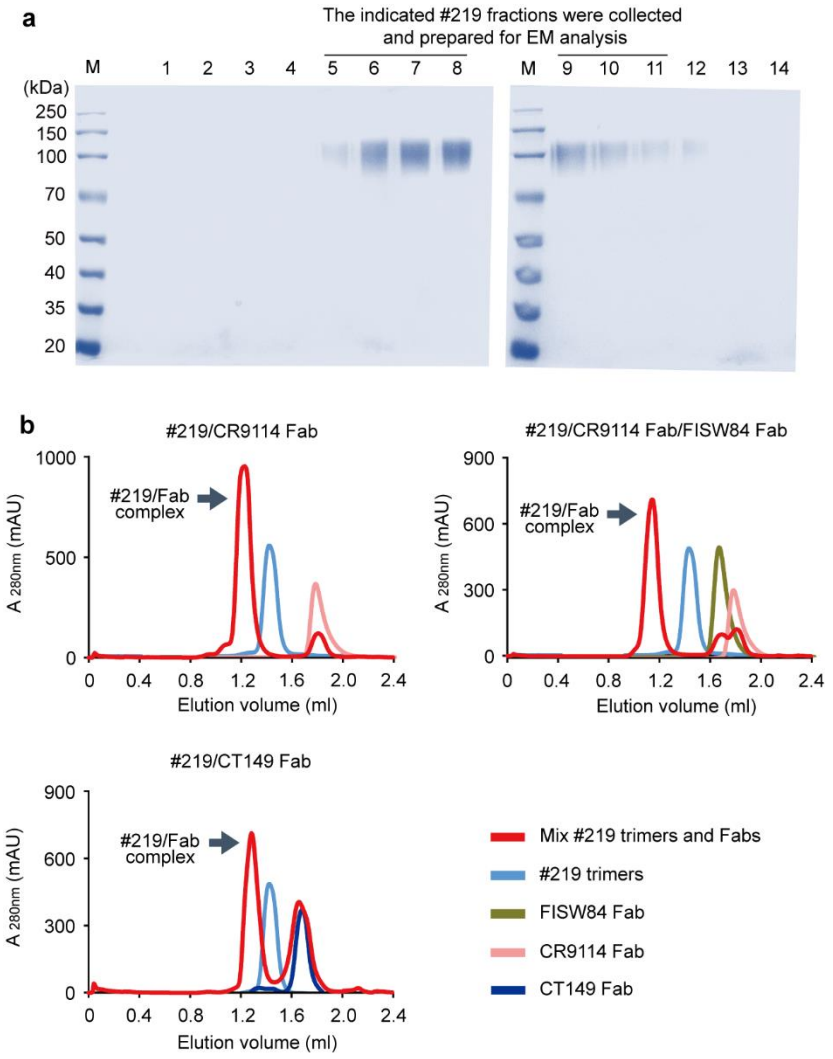

Extended Data Fig. 4. Preparation of high-purity #219 trimer protein and its complexes with Fabs. a, The affinity-purified #219 protein samples were fractionated by SEC. Fourteen fraction samples collected within the elution volume range from 12 ml to 14.8 ml were subjected to SDS-PAGE and Coomassie blue staining. The samples containing highly pure trimers of #219, as indicated by the black lines, were pooled and concentrated for the subsequent formation of various complexes of #219 and Fabs. The #219 trimers and the further purified #219/Fab complexes were subjected to EM analysis. **b**, The bindings of #219 to Fabs derived from bnAbs CR9114, CT149, and CR9114/FISW84 were analyzed through the means of SEC. All #219/Fabs complexes displayed a sharp peak, indicating a peak shift to a shorter retention time as indicated by arrows.

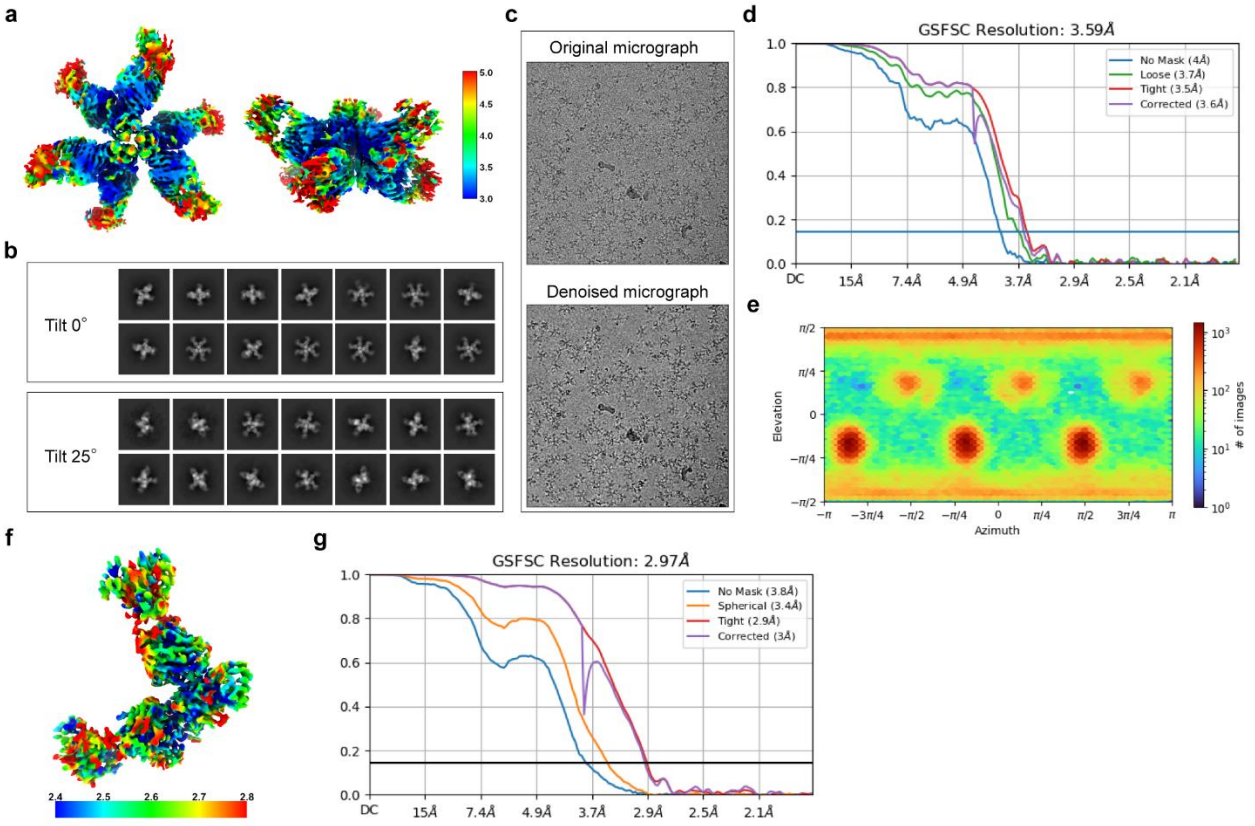

Extended Data Fig. 5. The cryo-EM data processing and validation. a, Local resolution (Å) was colored in the cryo-EM map of the #219/CR9114 Fab/FISW84 Fab immune complex. **b**, 2D class averages of the untilt and tilt of 25°. **c**, Micrographs before and after denoising by using the Topaz program. All micrographs underwent denoising before Topaz training. **d**, The resolution estimation of the immune complex using the Gold-standard (0.143) Fourier shell correlation method. A high-resolution map at 3.59 Å was reconstructed combining tilted data, effectively alleviating the preferred orientation challenge. **e**, The particle orientation distribution plot. **f**, Local resolution map of the monomer. **g**, The resolution estimation of the monomer by Gold-standard Fourier shell correlation method. Given that the trimer architecture of the immune complex has been validated, refinement efforts were directed towards the local focus of the asymmetric unit, resulting in an improved resolution of 2.97 Å.

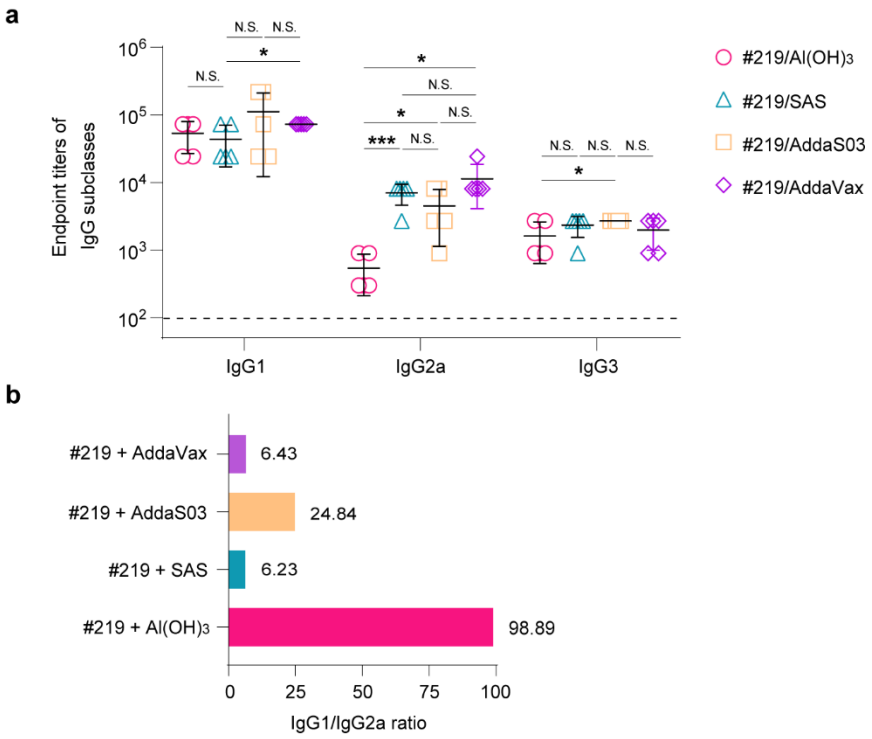

Extended Data Fig. 6. Serum IgG subclasses titers specific to NC99#2 H1. Serum samples were collected from mice two weeks after the second booster immunization. **a**, Endpoint titers of serum IgG1, IgG2a, and IgG3. **b**, IgG1/IgG2a ratios in immunization groups. The statistical analyses in panel (A) were performed using an unpaired two-tailed *t*-test. The symbols (*) indicate $p < 0.05$ and (***) $p < 0.005$. N.S. represents no significance.

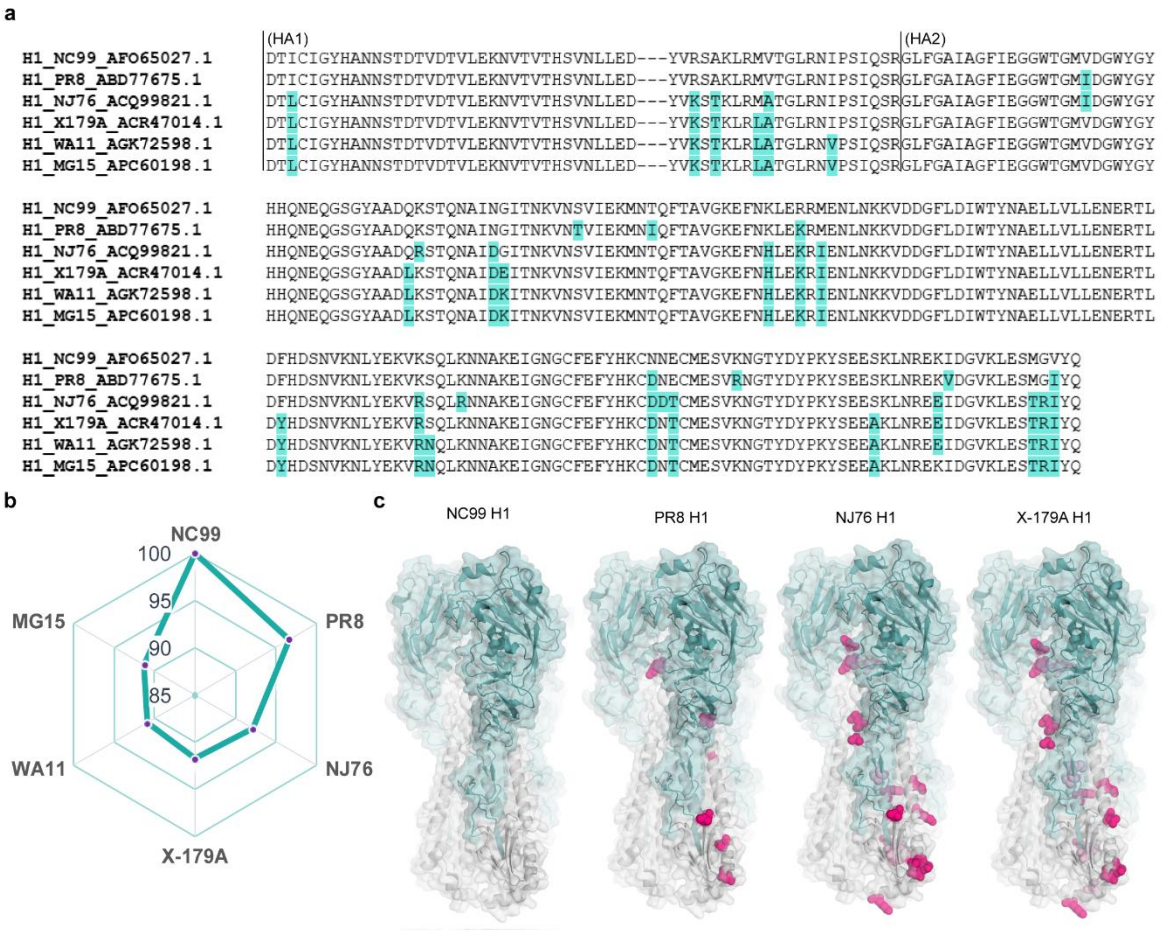

Extended Data Fig. 7. Identification of amino acid mutations in the stem domain of various H1 proteins. The sequence and structural model of the NC99 H1 stem are used as a reference template, because the #219 protein is designed based on it. **a**, Alignment of amino acid sequences derived from six H1 proteins which were contained in experimental materials in this study. Amino acid residues different from the NC99 H1-derived sequence are highlighted with blue teal color background. **b**, A radar chart depicting ratios of the number of unchanged residues to the total number of residues in the H1 sequences. The sequence from the PR8 H1 has fewer amino acid replacement than those of the other four H1. **c**, Structural models showing the mutated amino acid residues in the H1 stem domains of PR8, NJ76, and X-179A. These three virus strains were used for lethal infections of mice in viral challenge experiments. The FL NC99 H1 structure is displayed as ribbon and surface models (PDB ID: 7SCN). The mutated amino acid residues were represented by spheres, with those at the protein surface highlighted in hot pink, while those buried within the proteins were colored pink.

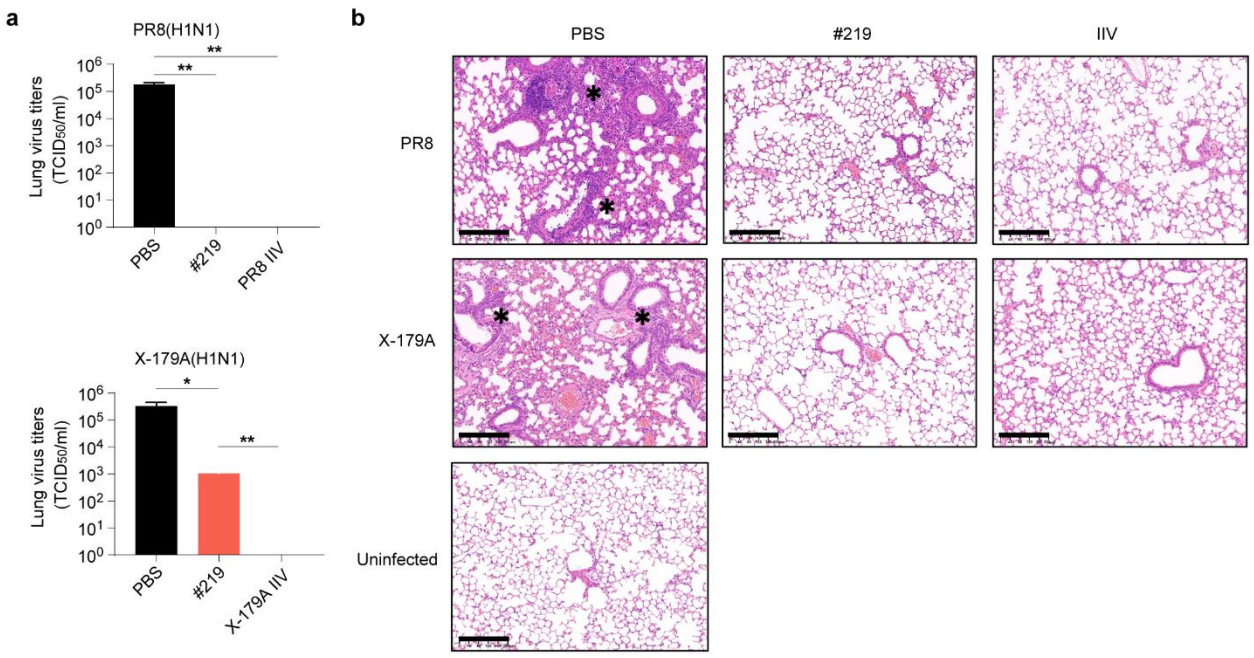

Extended Data Fig. 8. Histological analysis of mouse lung samples. Mouse lung samples were collected on the fifth day after sublethal infection with 1×LD_{50} PR8 or X-179A for **a**, lung virus titration and **b**, lung sectioning. (**a**) Data of lung virus titers are presented as mean ± SD (n = 3). Statistical analyses were performed using an unpaired two-tailed *t*-test. The symbols (*****) indicate $p < 0.05$ and (******) $p < 0.01$. (**b**) Ten μm-thick lung sections were prepared and stained using hematoxylin and eosin. A representative slide from each group is shown. The scale bars represent 200 nm. Asterisks denote areas of bronchial infiltration with immune cells.

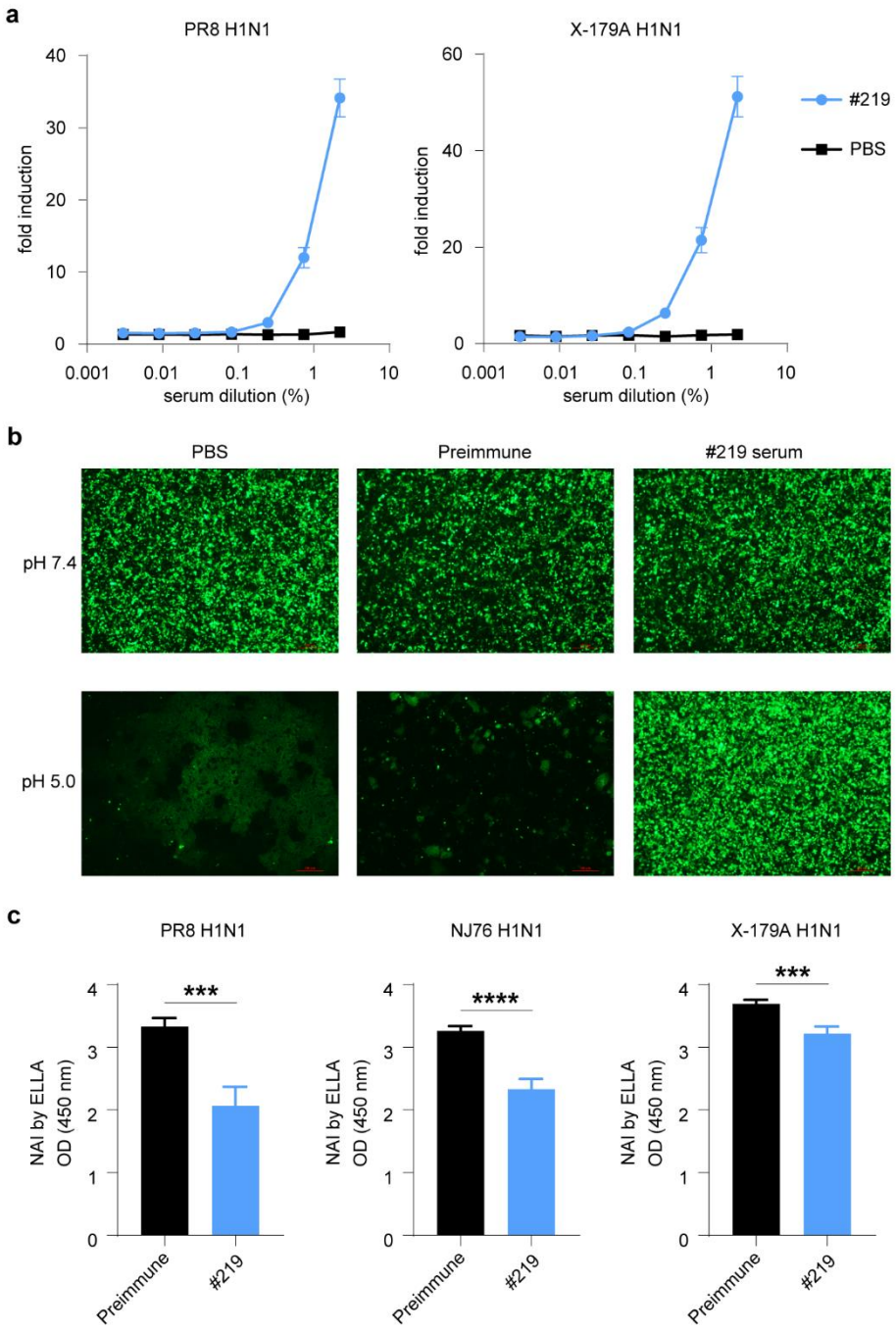

Extended Data Fig. 9. Mechanistic correlates of protection against influenza A virus. a, Serum ADCC activity to target cells infected with PR8 or X-179A. **b**, The #219 immune serum inhibited HA-mediated cell-cell fusion triggered by a low pH of 5.0. HA of the NC99 H1N1 virus and GFP were expressed in 293T cells. Cells treated with #219 immune serum, preimmune serum, or sterile PBS were challenged by pH 5.0. Scale bars represent 100 μm. Experiments were repeated twice. **c**, Inhibitory effect on viral neuraminidase. Data are presented as mean ± SD (n = 4), and statistical analyses of optical density (450 nm) values were performed using an unpaired two-tailed *t*-test. The symbols (***) indicate $p < 0.005$ and (****) $p < 0.001$.

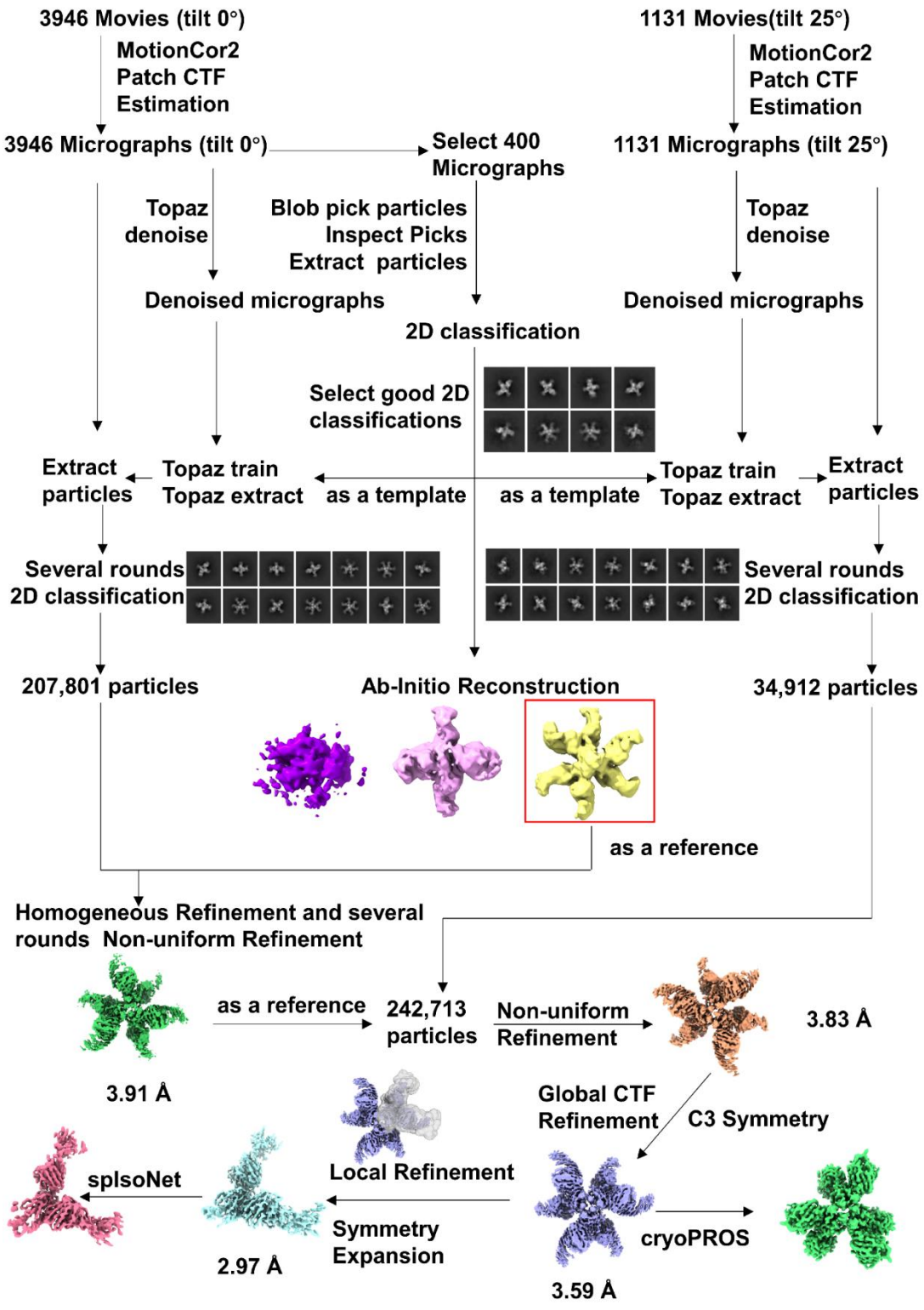

Extended Data Fig. 10. The cryo-EM data processing workflow for the structure of the #219/CR9114 Fab/FISW84 Fab immune complex. A total of 3,947 movies and 1,131 movies with a stage tilt of 25° were recorded. Motion between frames in each movie was corrected using the MotionCor2 program and was averaged into a single micrograph. Then, defocus of all

micrographs was estimated by patch CTF in the cryoSPARC. A set of particles were picked by Blob pick method from the selected 400 micrographs to generate high signal-to-noise (SNR) 2D classes as templates for particle picking in all denoised micrographs that were made by the Topaz denoising program. In addition, these high SNR particles filtered by (2D and 3D) classification method were used to reconstruct a 3D reference map. All particles from all micrographs were classified by the same way to obtain high SNR particles, followed by processes of non-uniform refinement and global Contrast Transfer Function (CTF) refinement with imposed C3 symmetry, reconstructed a map of 3.59 Å. A higher resolution (2.97 Å) map of the asymmetric unit reconstructed by employing symmetry expansion and local refinement. Finally, the spIsoNet and cryoPROS programs were utilized to address the preferred orientation problem.

Extended Data Table 1. The equilibrium dissociation constant (K_D) between #219 and the bnAbs.

Antibody types	K_D (nM)	K_{on} ($M^{-1}s^{-1}$)	K_{off} (s^{-1})	Full R^2
CR9114 IgG	0.033	1.27×10^{6}	4.13×10^{-5}	0.9942
CR6261 IgG	0.100	8.8×10^{5}	8.84×10^{-5}	0.9988
3I14 IgG	0.133	6.21×10^{5}	8.28×10^{-5}	0.9964
CT149 IgG	4.660	9.8×10^{5}	4.56×10^{-3}	0.9946

Extended Data Table 2. Cryo-EM data collection, refinement and validation statistics.

	#219/CR9114 Fab/FISW84 Fab complex (EMDB-61145) (PDB 9J5L)
Data collection and processing	
Magnification	130K
Voltage (kV)	300
Flux (e-/pix/sce)	20
Frames per exposure	32
Electron exposure (e–/Å^2)	50
Pixel size (Å)	0.92
Defocus range (μm)	1.0-2.5
Micrographs collected	3,946
Final particle images (no.)	242,713
Trimer resolution at 0.143 FSC (Å)	3.59 Å
Map resolution range (Å)	2.0 to 6.0
Protomer resolution at 0.143 FSC (Å)	2.97 Å
Map resolution range (Å)	1.9 to 3.4
Refinement	
Initial model used	AlphaFold2 predict model
Model resolution (Å)	2.9
FSC threshold	0.143

Map sharpening *B* factor (Å^2)	111.2
Model composition	
Non-hydrogen atoms	5038
Protein residues	653
Ligands	3
B factors (Å^2)	
Protein	118.50
Ligand	165.85
R.m.s. deviations	
Bond lengths (Å)	0.005
Bond angles (°)	0.818
Validation	
MolProbity score	1.51
Clashscore	3.95
Poor rotamers (%)	0
Ramachandran plot	
Favored (%)	95.27
Allowed (%)	4.73
Disallowed (%)	0

Extended Data Table 3. Serum hemagglutination inhibition titers against influenza A viruses (4×HA).

Influenza virus strains	Sera groups					
	PBS	#219	QIV	PR8 IIV	NJ76 IIV	X-179A IIV
PR8 H1N1	<10	<10	<10	1280	40	<10
NJ76 H1N1	<10	<10	20	40	1280	160
X-179A H1N1	<10	<10	320	10	320	1280
SC09 H1N1	<10	<10	320	10	320	1280
HK68 H3N2	<10	<10	<10	<10	<10	<10
GZ89 H3N2	<10	<10	<10	<10	<10	<10

References

47 Lee, P. S., Zhu, X., Yu, W. & Wilson, I. A. Design and Structure of an Engineered Disulfide-Stabilized Influenza Virus Hemagglutinin Trimer. *J Virol* **89**, 7417-7420, doi:10.1128/JVI.00808-15 (2015).

48 Reed, L. J. & Muench, H. A Simple Method of Estimating Fifty Per Cent Endpoints. *American journal of Epidemiology* **27**, 5 (1938).

49 Tan, Y. Z. *et al.* Addressing preferred specimen orientation in single-particle cryo-EM through tilting. *Nat Methods* **14**, 793-796, doi:10.1038/nmeth.4347 (2017).

50 Deng, L. *et al.* Protection against Influenza A Virus Challenge with M2e-Displaying Filamentous Escherichia coli Phages. *PLoS One* **10**, e0126650, doi:10.1371/journal.pone.0126650 (2015).

51 Liu, D. J. *et al.* Boost immunizations with NA-derived peptide conjugates achieve induction of NA inhibition antibodies and heterologous influenza protections. *Cell Rep* **42**, 112766, doi:10.1016/j.celrep.2023.112766 (2023).